Precision half-life measurement of ^{11}C: The most precise mirror transition $\mathcal{F}t$ value

A. A. Valverde,[1,*] M. Brodeur,[1] T. Ahn,[1] J. Allen,[1] D. W. Bardayan,[1] F. D. Becchetti,[2] D. Blankstein,[1] G. Brown,[1]
D. P. Burdette,[1] B. Frentz,[1] G. Gilardy,[1,3] M. R. Hall,[1] S. King,[1,4] J. J. Kolata,[1] J. Long,[1] K. T. Macon,[1] A. Nelson,[1]
P. D. O'Malley,[1] M. Skulski,[1] S. Y. Strauss,[1] and B. Vande Kolk[1]

[1]*Department of Physics, University of Notre Dame, Notre Dame, Indiana 46556, USA*
[2]*Physics Department, University of Michigan, Ann Arbor, Michigan 48109, USA*
[3]*Centre d'Études Nucléaires de Bordeaux Gradignan, UMR 5797 CNRS/IN2P3 - Université de Bordeaux, F-33175 Gradignan, France*
[4]*Department of Physics, University of Surrey, GU2 7XH, United Kingdom*

Background: The precise determination of the $\mathcal{F}t$ value in $T = 1/2$ mixed mirror decays is an important avenue for testing the standard model of the electroweak interaction through the determination of V_{ud} in nuclear β decays. ^{11}C is an interesting case, as its low mass and small Q_{EC} value make it particularly sensitive to violations of the conserved vector current hypothesis. The present dominant source of uncertainty in the ^{11}C $\mathcal{F}t$ value is the half-life.

Purpose: A high-precision measurement of the ^{11}C half-life was performed, and a new world average half-life was calculated.

Method: ^{11}C was created by transfer reactions and separated using the TwinSol facility at the Nuclear Science Laboratory at the University of Notre Dame. It was then implanted into a tantalum foil, and β counting was used to determine the half-life.

Results: The new half-life, $t_{1/2} = 1220.27(26)$ s, is consistent with the previous values but significantly more precise. A new world average was calculated, $t_{1/2}^{\text{world}} = 1220.41(32)$ s, and a new estimate for the Gamow-Teller to Fermi mixing ratio ρ is presented along with standard model correlation parameters.

Conclusions: The new ^{11}C world average half-life allows the calculation of a $\mathcal{F}t^{\text{mirror}}$ value that is now the most precise value for all superallowed mixed mirror transitions. This gives a strong impetus for an experimental determination of ρ, to allow for the determination of V_{ud} from this decay.

I. INTRODUCTION

Precision nuclear measurements provide a powerful tool for testing the standard model. Specifically, precision studies of nuclear β decays offer a method of testing the unitarity of the Cabibbo-Kobayashi-Maskawa (CKM) quark mixing matrix [1,2]. The conserved vector current (CVC) hypothesis requires that the CKM matrix be unitary. If this is not the case, then it would either mean the CVC hypothesis is incomplete, indicating the presence of other interactions for the β decay, such as scalar, pseudoscalar, or tensor interactions alongside the vector and axial-vector ones, or indicate the presence of other physics beyond the standard model, such as additional generations of quarks [1]. The highest-precision test of the CKM matrix unitarity comes from the normalization of the top row, $|V_{ud}|^2 + |V_{us}|^2 + |V_{ub}|^2 = 1$, where V_{ij} is the probability amplitude of a transition between two quark mass eigenstates [1,2]. Only V_{ud} and V_{us} contribute significantly to this determination [3]. The V_{us} element can be calculated from kaon decays [4], and experiments have improved the precision and accuracy of this value significantly over the past few years [3,5,6].

V_{ud} can be studied through pion decays, neutron decays, superallowed Fermi $0^+ \rightarrow 0^+$ transitions, and mixed mirror transitions [1,2]. The most accurate value for V_{ud} comes from superallowed Fermi $0^+ \rightarrow 0^+$ transitions, with a precision of 2.2×10^{-4} reported in the most recent review [6]. Recent efforts (e.g., Refs. [7–12]) have focused on further improving the precision of the experimental values for its determination. A complementary method is desirable to serve as a check on the value obtained from superallowed Fermi decays. One such method is the study of superallowed mixed mirror decays [13,14]. Occurring between $T = 1/2$ isospin doublets in mirror nuclei, these transitions are mixed Fermi and Gamow-Teller decays.

Following the CVC hypothesis, the product of the corrected statistical rate function $\mathcal{F}$ and the partial half-life t should have the same value for all $T = 1/2$ superallowed mixed mirror decays. We can calculate $\mathcal{F}t^{\text{mirror}}$ for these transitions as [13]:

$$\mathcal{F}t^{\text{mirror}} = f_V t(1 + \delta_R')\left(1 + \delta_{NS}^V - \delta_C^V\right), \quad (1)$$

where f_V is the uncorrected statistical rate function of the vector interaction and the various δ's are small correction terms: δ_R' the nucleus-dependent radiative correction, δ_{NS}^V the nuclear structure correction, and δ_C^V the isospin symmetry breaking correction. $\mathcal{F}t^{\text{mirror}}$ is related to the V_{ud} element of

*avalverd@nd.edu

the CKM matrix by [13]:

$$\mathcal{F}t^{\mathrm{mirror}} = \frac{K}{G_F^2 V_{ud}^2} \frac{1}{|M_F^0|^2 C_V^2 (1 + \Delta_R^V)(1 + \frac{f_A}{f_V}\rho^2)}, \quad (2)$$

where $K/(\hbar c)^6 = 2\pi^3 \hbar \ln(2)/(m_e c^2)^5 = 8120.2776(9) \times 10^{-10}$ GeV^{-4} s [6], $G_F/(\hbar c)^3 = 1.16637(1) \times 10^{-5}$ GeV^{-2} is the Fermi constant [13], $\Delta_R^V = 2.361(38)\%$ is the transition-independent radiative correction [15], M_F^0 is the Fermi matrix element in the isospin limit, which for these $T = 1/2$ mirror β decays is $|M_F^0|^2 = 1$, and $C_V^2 = 1$ is the vector coupling constant [13]. The quantities f_A and f_V are the statistical rate functions for the axial-vector and vector parts of this interaction, respectively, and ρ is the Gamow-Teller-to-Fermi mixing ratio.

The precise determination of $\mathcal{F}t$ relies on four experimental quantities: f_A and f_V require the decay transition energy Q_{EC}; calculation of the partial half-life t relies on both the half-life, $t_{1/2}$, and the branching ratio for the particular transition; and ρ, which can be determined from the measurement of either the β asymmetry parameter A_β, the β-neutrino angular correlation $a_{\beta\nu}$, or the neutrino asymmetry parameter B_ν. Currently, ρ has only been experimentally determined for five nuclei of interest, with A_β having been used for ^{19}Ne [16], ^{29}P [17], and ^{35}Ar [18,19], B_ν for ^{37}K [20], and $a_{\beta\nu}$ for ^{21}Na [21]. Efforts are underway to expand this list, including measuring A_β in ^{23}Mg using versatile ion-polarized techniques online (VITO) at ISOLDE [22] and a new ion trapping experiment under development at the Nuclear Science Laboratory (NSL) at the University of Notre Dame [23]. In parallel, a new high-precision half-life measurement program for superallowed $T = 1/2$ mixed mirror decays is also underway at the NSL [24,25].

Of particular interest among these superallowed mixed decays is ^{11}C, due to its importance to the search for physics beyond the standard model. If there are additional interactions alongside the vector and axial-vector interactions of the CVC hypothesis, they would be present in the calculation as an additional term in the integrand of the statistical rate function of $(1 + \frac{\gamma b_F}{W})$. Here, W is the total electron energy in electron rest mass units, $\gamma = \sqrt{1 - (\alpha Z)^2}$, with Z the atomic number of the daughter nucleus and α the fine structure constant, and b_F is the Fierz interference term [26]. The latter is related to the ratio of scalar coupling or tensor coupling to vector coupling or axial-vector coupling, respectively [5]. As the lighter $T = 1/2$ mixed decay nuclei have smaller Q_{EC} values, and thus W values, their decays are most sensitive to physics beyond the standard model, though such sensitivity would be limited by the uncertainty on the determination of ρ. ^{11}C is the lightest such nucleus that undergoes β^+ decay. Since ^{11}C decays completely to the ^{11}B ground state, a branching ratio measurement is unnecessary, and a recent high-precision Q_{EC} value measurement [27] has made the half-life the largest remaining source of experimental uncertainty, other than the unmeasured ρ. Hence, we performed a new, higher-precision half-life measurement of ^{11}C.

II. EXPERIMENTAL METHOD

A ^{10}B^{4+} primary beam with an energy of 32.5 MeV was created using the NSL's FN tandem accelerator. The primary beam was impinged on a deuterium gas target, which produced ^{11}C through the ^{10}B$(d,n)^{11}$C reaction. The resulting rare isotope beam was then passed through the twin solenoid TwinSol [28] mass separator, selecting an 18 MeV ^{11}C^{6+} secondary beam.

The ^{11}C ions were implanted in a thick tantalum foil in the NSL's β-counting station [24,29], which consists of a circular aluminum chamber containing a rotating aluminum arm on which a tantalum foil was mounted for implantation. The measurement was then conducted following the procedure outlined in Refs. [24,25], with the primary beam turned off during the counting stage by deflecting it with a high-voltage kicker upstream of the FN tandem Van de Graaff accelerator. ^{11}C was implanted in the tantalum foil for 60 min (approximately three half-lives), and then the foil was rotated into the counting position and the decay was measured. The individual betas were counted using a 1 mm plastic scintillator mounted to a light guide that was cemented to the photomultiplier tube. The photomultiplier tube used was an ET-Enterprises 9266QKSB, featuring a quartz window to minimize background from radioactive material and a mu-metal® shield, mounted to a high-pulse linearity RB1108 base. A thin [8(2) μm], light-tight aluminum foil was placed in front of the plastic scintillator; the thickness of the aluminum foil was minimized to maximize the recorded βs from the ^{11}C decay, which have a $Q_{\beta^+} = 1981.69(6)$ keV [30]. A series of nine implantations and half-life measurements were conducted in this way, varying the photomultiplier tube bias, discriminator threshold, and beam current (and thus initial count rate) between individual measurement runs in order to probe possible systematic effects.

III. DATA ANALYSIS

The data analysis followed the well-established procedure outlined in Ref. [31] as used previously in half-life measurements at the University of Notre Dame [24,25]. Each experimental run consisted of a single cycle containing a decay measurement and one or more cycles containing background measurements taken during implantation, which were then accounted for. Each remaining cycle contained between 1.9×10^6 and 11.1×10^6 total detected counts, taken over 220 minutes for the first run (approximately 11 half-lives) and 380 minutes (approximately 19 half-lives) for the remaining runs. The leading bins were excluded to avoid bins with anomalously low counts, and the data was rebinned to avoid the presence of a large number of empty bins, which could introduce a bias into the fit [25]. The initial 6600 and 11400 bins were rebinned to 600 bins, selected to optimize the χ_ν^2 of the fit.

A. Half-life determination

The ^{11}C data was fit using the summed fit procedure, as described in Ref. [31]. As the final eight measurements had the same cycle lengths, they could be combined into a single data set and considered as a whole; as the first run had a different
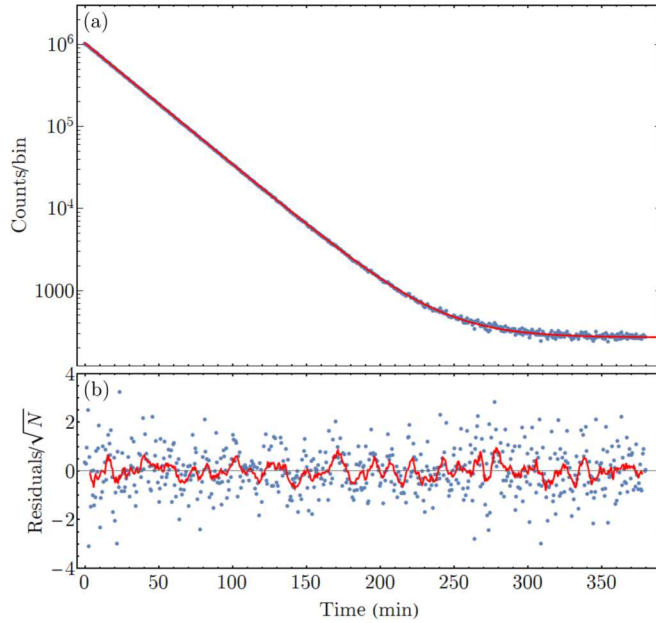
FIG. 1. (a) Summed β decay curves for runs 2–9 together with the fitted curve (red; solid). (b) Residuals divided by the square root of the fit number of counts in a given bin N and a ten-point moving average (red; solid). Each bin is 38 s wide.

cycle length, it was fit alone. In this analysis, the number of counts in each of the 600 bins of a run were adjusted for the dead-time losses inherent in the system [31]. These data were then fitted for the observed decay rate, $r(t)$, using:

$$r(t) = r_0 \exp\left[-\ln(2)t/t_{1/2}\right] + b, \qquad (3)$$

where r_0 is the initial rate, $t_{1/2}$ is the half-life, and b the background rate.

The fit used a maximum-likelihood-type fitting, where the Poisson maximum likelihood was approached iteratively through least-squares fitting using the Levenberg-Marquart algorithm. This was stopped once variation in all parameters was below 0.01% [31]. A cross check was performed using a second common approach [32], where the fit is determined by minimizing a χ^2 determined from Poisson statistics. Both methods yielded results identical to a few parts in 10^6. The summed fit and corresponding residuals of the dead-time corrected data for the combined runs 2–9 can be seen in Fig. 1. The reduced χ_ν^2 equals 1.04 and residuals average -0.004 with a standard deviation of 0.932. The absence of a nonstatistical trend, as shown by the ten-point moving average in the bottom panel of Fig. 1, indicates the absence of time-dependent systematic effects such as non-negligible contamination or improper accounting for dead time.

The resulting half-life from the summed fit was $t_{1/2} = 1221.38(89)$ s for the first run, and $t_{1/2} = 1220.20(22)$ s for the summed fit of runs 2 through 9. These values are consistent with each other, and have a weighted average of $t_{1/2} = 1220.27(22)$ s.
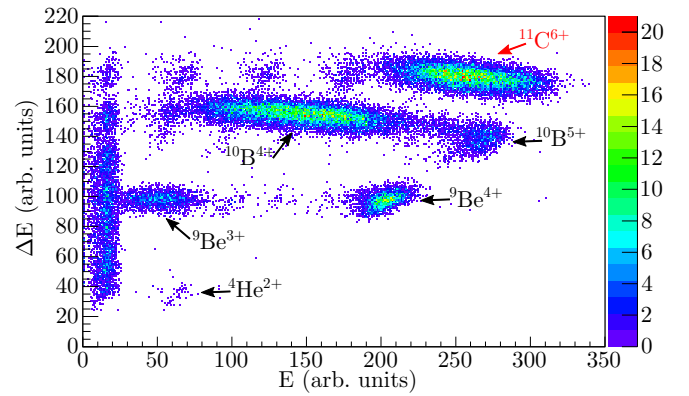

FIG. 2. Particle identification plot of the incoming cocktail beam separated by the TwinSol facility near the location of the β-counting station, showing energy lost in the first section of the ion chamber vs residual energy lost in the rest of the ion chamber. Faint periodic groups can be seen alongside the identified isotope groups, which are the result of interactions with the wires of the chamber.

B. Uncertainty estimation

Sources of uncertainty in both the measurement and the fitting procedure were considered. Among these are the possible presence of contaminants, the uncertainty in the dead time, and other sources of systematic error.

1. Contaminant-related considerations

An ion chamber was used to study the composition of the cocktail beam emerging from the TwinSol separator. The resulting particle identification plot, Fig. 2, shows no radioactive isotopes beyond the ^{11}C, and the heaviest isotopes produced were beryllium, boron, and carbon. Thus, heavier radioactive isotopes of nitrogen or oxygen were not produced and could not be contaminants. The energy of the primary beam was selected such that the production of other radioisotopes via ^{10}B-deuterium reactions was energetically forbidden, with the exception of long-lived ^{7}Be and ^{3}H. The beryllium only decays via electron capture, and the β decay of tritium is too low energy to pass the aluminum foil in front of the detector. Moreover, the 12-year half-life of tritium would have minimally affected our background. Nevertheless, fits for the observed decay rate $r(t)$ with two decaying half-lives were conducted, using:

$$r(t) = r_0\{\exp\left[-\ln(2)t/t_{1/2}\right] + \alpha \exp\left[-\ln(2)t/t_2\right]\} + b, \qquad (4)$$

where r_0, $t_{1/2}$ and b are defined as in Eq. (3), t_2 is the half-life of the possible contaminant, and α is the contamination ratio. With a free-floating t_2, this fit resulted in $t_2 = 2 \times 10^3 (3 \times 10^7)$ min and $\alpha = 4 \times 10^{-10}(5 \times 10^{-5})$; fixing t_2 as half or double that of ^{11}C result in $\alpha = 3 \times 10^{-9}(3 \times 10^{-3})$ and $\alpha = 6 \times 10^{-10}(2 \times 10^{-4})$, respectively, all of which are consistent with zero. We also investigated the possibility of a much longer-lived contaminant produced by the activation of the beam line. Such an activation is rendered extremely unlikely due to the 18 MeV energy of the secondary beam being below the Coulomb barrier for reactions with the nuclei in the primary

components of the stainless steel beamline, though it is possible on the aluminum of the paddle holding the tantalum foil; this would be a very small area exposed to an incident rate of less than 10^4 pps. The beam is turned off during the counting phase to further reduce the dose to the aluminum, and the counting station itself is located 12 m from the production target and separated from it by a 1.5 m thick high-density concrete wall, resulting in an immeasurably small neutron flux. Nevertheless, the possibility for the production of a long-lived contaminant polluting the spectra was probed by adding linear dependence of slope m to our background:

$$r(t) = r_0 \exp\left[-\ln(2)t/t_{1/2}\right] + mt + b, \qquad (5)$$

where m is the slope from the decay of the very long-lived contaminant. For this last fit, we found a slope $m = -0.002(40)$ s^{-1}, which is consistent with zero.

Possible short-lived contaminants and the possible misevaluation of the dead time were studied through removing the leading bins one by one and then performing a summed half-life fit on the remaining data. Up to the first 220 minutes were removed, corresponding to approximately eleven half-lives and over 99.8% of the total counts; any further removal of data does not result in a meaningful fit. As can be seen in Fig. 3, no time-dependent systematic trends are apparent in either the full data set or in the two subsets with varying initial count rates.

2. Dead-time uncertainty

The uncertainty in the dead time, $\tau = 56.89(9)$ μs, also affects the ^{11}C half-life. Hence, the summed fit was repeated using the two 1σ limits of τ, $\tau = 56.80$ and $\tau = 56.98$ μs, for these data. Half the difference between the weighted averages for these two cases, 0.14 s, was taken as the systematic uncertainty.

3. Other systematic effects

The 100 Hz clock frequency is known to be accurate to within 0.4 mHz. The summed fit was repeated using the extrema of the clock value, and the difference in half-life was found to be on the order of milliseconds. The effect of rebinning the data was recently explored using Monte-Carlo-generated data [25], which showed no systematic effects above the statistical uncertainty provided few bins had zero counts; the difference in half-life between rebinning into 200 and 1000 bins is on the order of hundredths of seconds. Both of these have been considered as sources of systematic uncertainty.

To search for other possible systematic effects, the photomultiplier tube bias voltage, discriminator threshold voltage, and beam current were all varied. The photomultiplier tube was biased at 1000 and 1100 V, the discriminator set at 0.3 and 0.5 V, and the primary beam current was varied resulting in initial β-count rates ranging from 1500–10500 per second. The background varied from 0.3 to 1.6 counts/s on individual runs, depending on the PMT bias and threshold voltage. Combinations of these parameters were explored in each run, and the fitting procedure was performed individually to probe systematics. As can be seen in the top panel of Fig. 4, there are no apparent systematic effects; the absence of any rate-
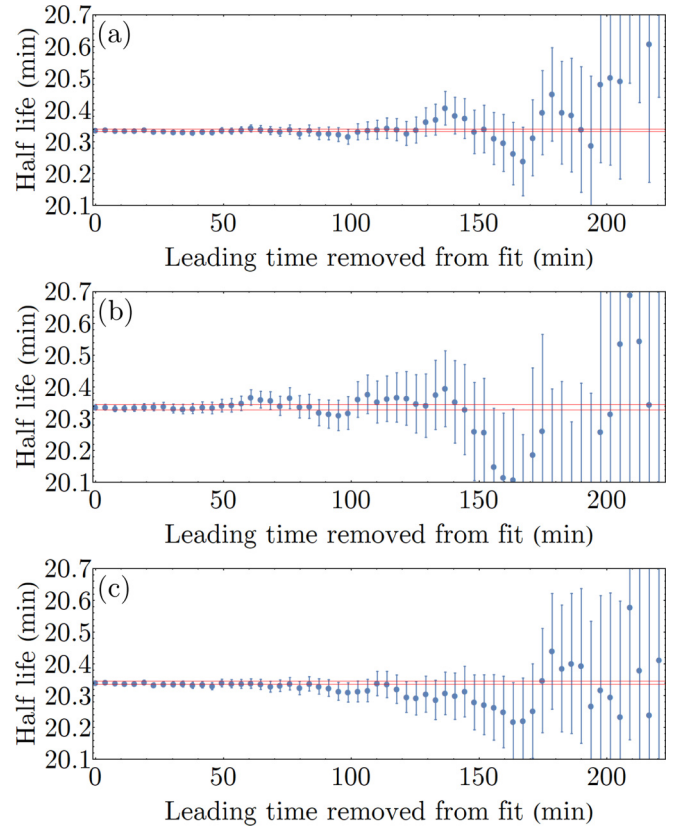

FIG. 3. Fitted half-lives for the summed data as a function of the leading time removed. The two horizontal (red) lines are the uncertainty on the half-life without any bin removal. (a) represents the sum of all eight same-length runs, (b) the sum of the three runs with an initial count rate of approximately 3000 counts per second, and (c) the sum of the two runs with an initial count rate of approximately 10000 counts per second.

dependent effects here or in Fig. 3 further indicates that there are no rate-dependent photomultiplier tube gain shifts [33]. This was tested through 100 different Monte-Carlo-simulated data sets with the same initial rates and background as the experimental data sets. As indicated by the Monte-Carlo-generated sample data set at the bottom panel of Fig. 4, a similar scatter between the experimental and simulated data sets is observed. Furthermore, as indicated by the shaded region on the bottom panel of Fig. 4, the one standard deviation spread calculated from the 100 simulated data sets overlaps with the spread in the data.

The weighted average of these individual runs gives a half-life of $t_{1/2} = 1220.24(22)$ s, which is in agreement with the value from the sum fit. The small, 26 ms difference can be explained by a bias of the maximum likelihood fitting with count rate [31], and is replicated in the 36 ms average spread from the 100 Monte-Carlo-generated data sets. Nevertheless, half of the experimental difference is added as a systematic uncertainty. The Birge ratio [34] of these measurements, 0.95(16), indicates that the variation in values is statistical in nature. Finally, the accuracy of the sum fitting was tested by taking the weighted average of the sum fits for each of the 100 Monte-Carlo-generated data sets. The
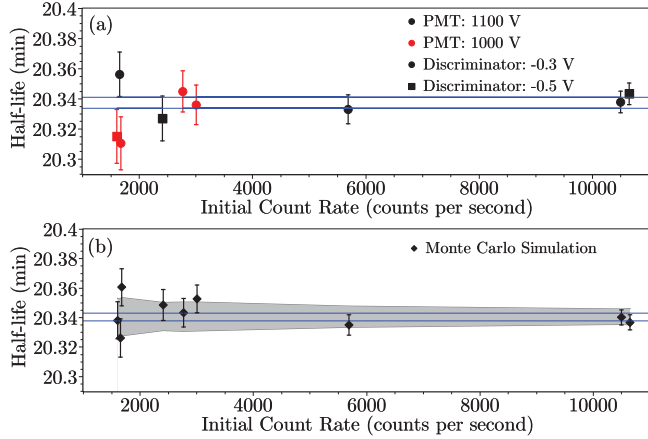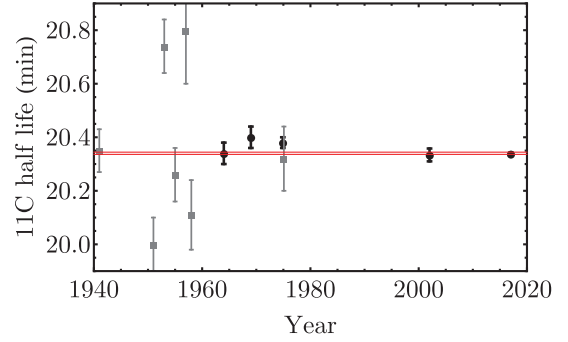
FIG. 5. Half-lives of ^{11}C considered in the calculation of the new world average [35–38] (black circles), as well as those considered previously and now eliminated [39–45] (gray squares). The horizontal (red) lines represent the uncertainty on $t_{1/2} = 1220.41(32)$ s.

[3,13]. This leaves four earlier values that are used to calculate the new world average (Refs. [35–38]). These, alongside our new measurement, can be seen in Fig. 5. A weighted average of the five measurements was taken, giving a world average of $t_{1/2}^{\mathrm{world}} = 1220.41(32)$ s, which is a factor of five more precise than the previous value. The Birge ratio of our new average is 1.28(21), an improvement on the previous value of 2.06(14). As it is greater than one, we adopt the policy of the Particle Data Group [46], and the uncertainty reported on the world average has been scaled by the Birge ratio.

V. DISCUSSION

Using our new world average half-life and the recent value for f_V from [27], we can now calculate a new value for $\mathcal{F}t^{\mathrm{mirror}}$ following Eq. (1). A summary of the values used in this calculation and their sources can be seen in Table II. Our new value is an improvement of a factor of 2.6 in the uncertainty over the previous value. This now makes the ^{11}C $\mathcal{F}t^{\mathrm{mirror}}$-value the most precise to date, with a level of precision comparable to the most precise $\mathcal{F}t^{0^+ \to 0^+}$ values.

This new $\mathcal{F}t^{\mathrm{mirror}}$ value allows us to extract a standard model prediction for ρ using the world average $\mathcal{F}t^{0^+ \to 0^+}$, obtained from the 14 most precise Fermi superallowed $0^+ \to 0^+$ decays [6]. Using $|M_f^0|^2 = 1$ for $T = 1/2$ mirror decays and $|M_f^0|^2 = 2$ for the pure Fermi $T = 1$ decays, we can determine from

---

FIG. 4. (a) Half-life results from fitting individual samples vs initial count rate. Point color indicates the photomultiplier tube voltage, and shape indicates discriminator voltage. The two horizontal (blue) lines are the uncertainty on the weighted average of these values. (b) Monte-Carlo-simulated data of the same varying rates, showing the same statistical scatter around the weighted average half-life, indicated by two horizontal (blue) lines. The gray band indicates the 1σ spread of 100 such simulations.

difference of $-11(18)$ ms with the input half-life, which is consistent with zero, demonstrates the accuracy of the fitting technique. Nevertheless, to be conservative, an uncertainty of 18 ms is added as a systematic uncertainty. The statistical and systematic uncertainties, summarized in Table I, are then combined in quadrature, resulting in a total uncertainty of 0.26 s.

IV. ^{11}C HALF-LIFE

Our new half-life value, $t_{1/2} = 1220.27(26)$ s, is in good agreement with the previous world average, $t_{1/2}^{\mathrm{old}} = 1221.6(1.5)$ s, but is significantly more precise. Following the same procedure used for previous reviews of superallowed mixed mirror decays [13] and superallowed pure Fermi $0^+ \to 0^+$ decays [3], we reevaluated the world data in order to calculate a new world average half-life. As our new value is significantly more precise than the previous values, seven of those used in the previous evaluation (Refs. [39–45]) were eliminated, being more than ten times less precise, following the established procedure

TABLE I. Summary of statistical and systematic uncertainties combined to give final uncertainty.

Source	Uncertainty (s)
Statistical	0.22
Dead-time uncertainty	0.14
Binning	0.026
Fit (Monte Carlo)	0.018
Fit (individual vs. sum)	0.013
Clock uncertainty	0.005
Fit ([31] vs. [32])	0.004
Total	0.26

TABLE II. Parameters used in calculation of $\mathcal{F}t^{\mathrm{mirror}}$ and related values in this work.

Ref.	Parameter	Value
This work	$t_{1/2}^{\mathrm{world}}$	1220.41(32) s
Gulyuz *et al.* [27]	Q_{EC}	1981.690(61) keV
Gulyuz *et al.* [27]	f_V	3.1829(8)
This work	f_A	3.2163(8)
Severijns *et al.* [13]	δ_R'	1.660(4)%
Severijns *et al.* [13]	$\delta_C^V - \delta_{NS}^V$	1.04(3)%
Hardy and Towner [6]	$\mathcal{F}t^{0^+ \to 0^+}$	3072.27(72) s

TABLE III. Comparison of calculated values from this work to Gulyuz *et al.* [27].

Parameter	This work	Gulyuz *et al.* [27]
$\mathcal{F}t^{\text{mirror}}$	3916.9(1.9) s	3920.4(5.0) s
ρ	0.75022(56)	0.7493(15)
a_{SM}	0.51982(46)	0.5206(13)
A_{SM}	$-0.59962(2)$	$-0.59959(5)$
B_{SM}	$-0.8877(3)$	$-0.8872(8)$

Eq. (2) [13] that:

$$\mathcal{F}t^{\text{mirror}} = \frac{2\mathcal{F}t^{0^+ \to 0^+}}{1 + \frac{f_A}{f_V}\rho^2}, \tag{6}$$

where f_A was calculated from the Q_{EC} in Ref. [27] and the parametrization presented in Ref. [47]. This was then solved for ρ, and this value, as well as the correlation coefficients A_{SM}, a_{SM}, and B_{SM}, was calculated following the standard model [13]. As in Ref. [13], our calculated correlation coefficients at $E_\beta = 0$ include neither physics beyond the standard model nor recoil order effects, which would affect measured correlation coefficients. These results can be seen in Table III, showing significant factors of three to five improvement over the previous results.

VI. OUTLOOK

In summary, we have improved the precision of the measured world average half-life of ^{11}C, the lightest and longest-lived superallowed mixed mirror β^+ decay, by a factor of five, making it comparable in precision to the Q value and thus increasing the precision of the $\mathcal{F}t^{\text{mirror}}$ value fourfold. In examining the fractional contributions to the final uncertainty of the $\mathcal{F}t^{\text{mirror}}$ value, Fig. 6, we can see that the largest uncertainty now comes from the theoretical $\delta_{NS}^V - \delta_C^V$ correction,
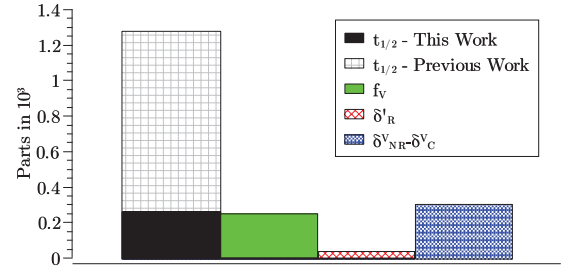

FIG. 6. Fractional contribution of experimental and theoretical parameters to the final uncertainty in $\mathcal{F}t^{\text{mirror}}$.

providing an impetus for improved precision calculations. The new estimate for ρ and the related standard model correlation coefficients also show a factor of three to five improvement over the previous results.

The high precision achieved on the $\mathcal{F}t^{\text{mirror}}$ value is now the most accurate of any superallowed mixed mirror decay and is comparable in precision to the most precise $\mathcal{F}t^{0^+ \to 0^+}$ values. With this measurement, it would only take a relative precision of 0.5% on a measurement of ρ to determine V_{ud} with a relative uncertainty of 0.2%, comparable to the uncertainties on Fermi superallowed decays that currently provide the most precise determinations of V_{ud} [6]. This, and the high sensitivity of low-Z decays to physics beyond the standard model, provides a strong impetus for efforts to measure the correlation coefficients, such as the planned Paul trap for measuring $a_{\beta\nu}$ at the NSL at the University of Notre Dame [23].

ACKNOWLEDGMENTS

[1] N. Severijns and O. Naviliat-Cuncic, Annu. Rev. Nucl. Part. Sci. **61**, 23 (2011).

[2] J. C. Hardy and I. S. Towner, Ann. Phys. (NY) **525**, 443 (2013).

[3] J. C. Hardy and I. S. Towner, Phys. Rev. C **71**, 055501 (2005).

[4] O. Naviliat-Cuncic and M. González-Alonso, Ann. Phys. (NY) **525**, 600 (2013).

[5] J. C. Hardy and I. S. Towner, Phys. Rev. C **79**, 055502 (2009).

[6] J. C. Hardy and I. S. Towner, Phys. Rev. C **91**, 025501 (2015).

[7] M. R. Dunlop, C. E. Svensson, G. C. Ball, G. F. Grinyer, J. R. Leslie, C. Andreoiu, R. A. E. Austin, T. Ballast, P. C. Bender, V. Bildstein, A. D. Varela, R. Dunlop, A. B. Garnsworthy, P. E. Garrett, G. Hackman, B. Hadinia, D. S. Jamieson, A. T. Laffoley, A. D. MacLean, D. M. Miller, W. J. Mills, J. Park, A. J. Radich, M. M. Rajabali, E. T. Rand, C. Unsworth, A. Valencik, Z. M. Wang, and E. F. Zganjar, Phys. Rev. Lett. **116**, 172501 (2016).

[8] P. A. Voytas, E. A. George, G. W. Severin, L. Zhan, and L. D. Knutson, Phys. Rev. C **92**, 065502 (2015).

[9] A. A. Valverde, G. Bollen, M. Brodeur, R. A. Bryce, K. Cooper, M. Eibach, K. Gulyuz, C. Izzo, D. J. Morrissey, M. Redshaw, R. Ringle, R. Sandler, S. Schwarz, C. S. Sumithrarachchi, and A. C. C. Villari, Phys. Rev. Lett. **114**, 232502 (2015).

[10] A. A. Kwiatkowski, A. Chaudhuri, U. Chowdhury, A. T. Gallant, T. D. Macdonald, B. E. Schultz, M. C. Simon, and J. Dilling, Ann. Phys. (NY) **525**, 529 (2013).

[11] A. T. Laffoley, C. E. Svensson, C. Andreoiu, R. A. E. Austin, G. C. Ball, B. Blank, H. Bouzomita, D. S. Cross, A. Diaz Varela, R. Dunlop, P. Finlay, A. B. Garnsworthy, P. E. Garrett, J. Giovinazzo, G. F. Grinyer, G. Hackman, B. Hadinia, D. S. Jamieson, S. Ketelhut, K. G. Leach, J. R. Leslie, E. Tardiff, J. C. Thomas, and C. Unsworth, Phys. Rev. C **88**, 015501 (2013).

[12] T. Eronen, D. Gorelov, J. Hakala, J. C. Hardy, A. Jokinen, A. Kankainen, V. S. Kolhinen, I. D. Moore, H. Penttilä, M. Reponen, J. Rissanen, A. Saastamoinen, and J. Äystö, Phys. Rev. C **83**, 055501 (2011).

[13] N. Severijns, M. Tandecki, T. Phalet, and I. S. Towner, Phys. Rev. C **78**, 055501 (2008).

[14] O. Naviliat-Cuncic and N. Severijns, Phys. Rev. Lett. **102**, 142302 (2009).

[15] W. J. Marciano and A. Sirlin, Phys. Rev. Lett. **96**, 032002 (2006).

[16] F. P. Calaprice, S. J. Freedman, W. C. Mead, and H. C. Vantine, Phys. Rev. Lett. **35**, 1566 (1975).

[17] G. S. Masson and P. A. Quin, Phys. Rev. C **42**, 1110 (1990).

[18] J. D. Garnett, E. D. Commins, K. T. Lesko, and E. B. Norman, Phys. Rev. Lett. **60**, 499 (1988).

[19] A. Converse, M. Allet, W. Haeberli, W. Hajdas, J. Lang, J. Liechti, H. Lüscher, M. Miller, R. Müller, O. Naviliat-Cuncic, P. Quin, and J. Sromicki, Phys. Lett. B **304**, 60 (1993).

[20] D. Melconian, J. Behr, D. Ashery, O. Aviv, P. Bricault, M. Dombsky, S. Fostner, A. Gorelov, S. Gu, V. Hanemaayer, K. Jackson, M. Pearson, and I. Vollrath, Phys. Lett. B **649**, 370 (2007).

[21] P. A. Vetter, J. R. Abo-Shaeer, S. J. Freedman, and R. Maruyama, Phys. Rev. C **77**, 035502 (2008).

[22] M. Deicher, M. Stachura, V. Amaral, M. Bissell, J. Correia, A. Gottberg, L. Hemmingsen, S. Hong, K. Johnston, Y. Kadi, M. Kowalska, J. Lehnert, A. Lopes, G. Neyens, K. Potzger, D. Pribat, N. Severijns, C. Tenreiro, P. Thulstrup, T. Trindade, T. Wichert, H. Wolf, D. Yordanov, and Z. Salman, *VITO - Versatile Ion-polarized Techniques On-line at ISOLDE (former ASPIC UHV beamline)*, Technical Report CERN-INTC-2013-013. INTC-O-017 (CERN, Geneva, 2013), http://cds.cern.ch/record/1551750.

[23] M. Brodeur, J. Kelly, J. Long, C. Nicoloff, and B. Schultz, Nucl. Instrum. Methods B **376**, 281 (2016), proceedings of the XVIIth International Conference on Electromagnetic Isotope Separators and Related Topics (EMIS2015), Grand Rapids, Michigan, USA, 11–15 May, 2015.

[24] M. Brodeur, C. Nicoloff, T. Ahn, J. Allen, D. W. Bardayan, F. D. Becchetti, Y. K. Gupta, M. R. Hall, O. Hall, J. Hu, J. M. Kelly, J. J. Kolata, J. Long, P. O'Malley, and B. E. Schultz, Phys. Rev. C **93**, 025503 (2016).

[25] J. Long, T. Ahn, J. Allen, D. W. Bardayan, F. D. Becchetti, D. Blankstein, M. Brodeur, D. Burdette, B. Frentz, M. R. Hall, J. M. Kelly, J. J. Kolata, P. D. O'Malley, B. E. Schultz, S. Y. Strauss, and A. A. Valverde, Phys. Rev. C **96**, 015502 (2017).

[26] J. Jackson, S. Treiman, and H. Wyld, Nucl. Phys. **4**, 206 (1957).

[27] K. Gulyuz, G. Bollen, M. Brodeur, R. A. Bryce, K. Cooper, M. Eibach, C. Izzo, E. Kwan, K. Manukyan, D. J. Morrissey, O. Naviliat-Cuncic, M. Redshaw, R. Ringle, R. Sandler, S. Schwarz, C. S. Sumithrarachchi, A. A. Valverde, and A. C. C. Villari, Phys. Rev. Lett. **116**, 012501 (2016).

[28] F. D. Becchetti and J. J. Kolata (TwinSol Collaboration), Nucl. Instrum. Methods B **376**, 397 (2016), proceedings of the XVIIth International Conference on Electromagnetic Isotope Separators and Related Topics (EMIS2015), Grand Rapids, Michigan, USA, 11–15 May, 2015.

[29] T. Ahn, D. W. Bardayan, D. Bazin, S. Beceiro Novo, F. D. Becchetti, J. Bradt, M. Brodeur, L. Carpenter, Z. Chajecki, M. Cortesi, A. Fritsch, M. R. Hall, O. Hall, L. Jensen, J. J. Kolata, W. Lynch, W. Mittig, P. O'Malley, and D. Suzuki, Nucl. Instrum. Methods B **376**, 321 (2016), proceedings of the XVIIth International Conference on Electromagnetic Isotope Separators

and Related Topics (EMIS2015), Grand Rapids, Michigan, USA, 11–15 May, 2015.

[30] M. Wang, G. Audi, F. Kondev, W. Huang, S. Naimi, and X. Xu, Chin. Phys. C **41**, 030003 (2017).

[31] V. Koslowsky, E. Hagberg, J. Hardy, G. Savard, H. Schmeing, K. Sharma, and X. Sun, Nucl. Instrum. Meth. A **401**, 289 (1997).

[32] G. F. Grinyer, C. E. Svensson, C. Andreoiu, A. N. Andreyev, R. A. E. Austin, G. C. Ball, R. S. Chakrawarthy, P. Finlay, P. E. Garrett, G. Hackman, J. C. Hardy, B. Hyland, V. E. Iacob, K. A. Koopmans, W. D. Kulp, J. R. Leslie, J. A. Macdonald, A. C. Morton, W. E. Ormand, C. J. Osborne, C. J. Pearson, A. A. Phillips, F. Sarazin, M. A. Schumaker, H. C. Scraggs, J. Schwarzenberg, M. B. Smith, J. J. Valiente-Dobón, J. C. Waddington, J. L. Wood, and E. F. Zganjar, Phys. Rev. C **71**, 044309 (2005).

[33] S. Triambak, P. Finlay, C. S. Sumithrarachchi, G. Hackman, G. C. Ball, P. E. Garrett, C. E. Svensson, D. S. Cross, A. B. Garnsworthy, R. Kshetri, J. N. Orce, M. R. Pearson, E. R. Tardiff, H. Al-Falou, R. A. E. Austin, R. Churchman, M. K. Djongolov, R. D'Entremont, C. Kierans, L. Milovanovic, S. O'Hagan, S. Reeve, S. K. L. Sjue, and S. J. Williams, Phys. Rev. Lett. **109**, 042301 (2012).

[34] R. T. Birge, Phys. Rev. **40**, 207 (1932).

[35] T. M. Kavanagh, J. K. P. Lee, and W. T. Link, Can. J. Phys. **42**, 1429 (1964).

[36] M. Awschalom, F. Larsen, and W. Schimmerling, Nucl. Instrum. Methods **75**, 93 (1969).

[37] G. Azuelos and J. E. Kitching, Phys. Rev. C **12**, 563 (1975).

[38] D. H. Woods, M. I. Baker, J. D. Keightley, L. J. Keightley, J. L. Makepeace, A. K. Pearce, A. P. Woodman, M. J. Woods, S. A. Woods, and S. Waters, Appl. Radiat. Isotopes **56**, 327 (2002), proceedings of the Conference on Radionuclide Metrology and its Applications, ICRM'01.

[39] J. H. C. Smith and D. B. Cowie, J. Appl. Phys. **12**, 78 (1941).

[40] J. M. Dickson and T. C. Randle, Proc. Phys. Soc. London, Sect. A **64**, 902 (1951).

[41] D. N. Kundu, T. W. Donaven, M. L. Pool, and J. K. Long, Phys. Rev. **89**, 1200 (1953).

[42] W. C. Barber, W. D. George, and D. D. Reagan, Phys. Rev. **98**, 73 (1955).

[43] I. D. Prokoshkin and A. Tiapkin, Soviet Phys. JETP **5**, 148 (1957).

[44] S. Arnell, J. Dubois, and O. Almén, Nucl. Phys. **6**, 196 (1958).

[45] H. Behrens, M. Kobelt, L. Szybisz, and W.-G. Thies, Nucl. Phys. A **246**, 317 (1975).

[46] Particle Data Group, J. Beringer, J. F. Arguin, R. M. Barnett, K. Copic, O. Dahl, D. E. Groom, C. J. Lin, J. Lys, H. Murayama, C. G. Wohl, W. M. Yao *et al.*, Phys. Rev. D **86**, 010001 (2012).

[47] I. S. Towner and J. C. Hardy, Phys. Rev. C **91**, 015501 (2015).